



Published in final edited form as:

Oncogene. 2015 December 10; 34(50): 6040–6054. doi:10.1038/onc.2015.52.

YAP forms autocrine loops with the ERBB pathway to regulate ovarian cancer initiation and progression

Chunbo He^{1,2}, Xiangmin Lv¹, Guohua Hua^{1,2}, Subodh M Lele⁴, Steven Remmenga^{1,3}, Jixin Dong³, John S Davis^{1,3,5}, and Cheng Wang^{1,3}

¹Olson Center for Women's Health, Department of Obstetrics and Gynecology, University of Nebraska Medical Center, Omaha, NE 68198, USA

²College of Animal Sciences and Technology, Huazhong Agricultural University, Wuhan, Hubei province 430070, P.R.China

³Fred & Pamela Buffett Cancer Center, University of Nebraska Medical Center, Omaha NE 68198, USA

⁴Department of Pathology and Microbiology, University of Nebraska Medical Center, Omaha NE 68198, USA

⁵Omaha Veterans Affairs Medical Center, Omaha, NE 68105, USA

Abstract

Mechanisms underlying ovarian cancer initiation and progression are unclear. Herein, we report that the Yes-associated protein (YAP), a major effector of the Hippo tumor suppressor pathway, interacts with ERBB signaling pathways to regulate the initiation and progression of ovarian cancer. Immunohistochemistry studies indicate that YAP expression is associated with poor clinical outcomes in patients. Overexpression or constitutive activation of YAP leads to transformation and tumorigenesis in human ovarian surface epithelial cells, and promotes growth of cancer cells *in vivo* and *in vitro*. YAP induces expression of EGF receptors (EGFR, ERBB3) and production of EGF-like ligands (HBEGF, NRG1 and NRG2). HBEGF or NRG1, in turn, activates YAP and stimulates cancer cell growth. Knockdown of ERBB3 or HBEGF eliminates YAP effects on cell growth and transformation, while knockdown of YAP abrogates NRG1- and HBEGF-stimulated cell proliferation. Collectively, our study demonstrates the existence of HBEGF&NRGs/ERBBs/YAP/HBEGF&NRGs autocrine loop that controls ovarian cell tumorigenesis and cancer progression.

Users may view, print, copy, and download text and data-mine the content in such documents, for the purposes of academic research, subject always to the full Conditions of use:http://www.nature.com/authors/editorial_policies/license.html#terms

Corresponding Author: Cheng Wang, PhD, Olson Center for Women's Health, Department of OB/GYN, Fred & Pamela Buffett Cancer Center, University of Nebraska Medical Center, Omaha NE 68198-6265, ; Email: chengwang@unmc.edu, Tel: 402-559-8665, Fax: 402-559-1159

Conflict of interest: The authors have no competing interests to declare.

AUTHOR CONTRIBUTIONS

C.H. contributed to the design, performance, data analysis, and manuscript preparation. X.L. packaged the retrovirus and performed *in vivo* experiments. G.H. conducted IHC analysis. J.D. constructed the retroviral vectors. S.L. and S.R. evaluated and analyzed patient samples. J.S.D. contributed to the experimental design, results, discussion, and manuscript preparation. C.W. supervised these studies and contributed to the experimental design, data analysis, and manuscript preparation.

Keywords

YAP; Ovarian cancer; HBEGF; NRG1; EGFR; ERBB3

INTRODUCTION

According to an American Cancer Society estimate for the year 2014, approximately 21,980 new cases of ovarian cancer will be diagnosed and 14,270 women will die of this disease in the United States alone.¹ Despite decades of research and evolving treatment modalities, the five-year survival rate of ovarian cancer is still around 40%. However, if patients are diagnosed in early stages, when tumor cells are confined to ovary, the five-year survival rate rises to 94%.² The reality is that molecular markers or events that facilitate early diagnosis of ovarian cancer have not yet been established.

The Hippo pathway was initially described in *Drosophila*.^{3, 4} Subsequent studies have shown that the Hippo pathway is conserved among species.^{5, 6} Yes-associated protein (YAP1 or more commonly YAP) is a transcriptional co-activator and the pivotal effector of the Hippo pathway.^{5, 6} Suppression of the Hippo pathway or overexpression of YAP can lead to organ overgrowth and tumorigenesis in model organisms.^{5, 6} Recent studies have shown that YAP overexpression occurs in a broad range of human carcinomas, including lung, colorectal, breast, ovarian, pancreatic, gastric, and liver cancer,⁷⁻¹¹ although differing results have been observed.^{12, 13} Several groups have shown that YAP may play a role in the progression of ovarian cancer;^{9, 10, 14} however, the relationships among YAP expression and clinicopathological outcomes in ovarian cancer are under debate.^{9, 10, 14} Thus, the role and functional mechanism of YAP on ovarian tumorigenesis and ovarian cancer progression are not fully understood.

The actin cytoskeleton or cellular tension appears to be the master mediator that integrates and transmits upstream signals to the core Hippo signaling cascade.^{6, 15} It has been proposed that activation of epidermal growth factor receptors (EGFR) promotes cell growth by changing cell polarity, affecting cell mechanotransduction and overcoming cell contact inhibition.¹⁶⁻¹⁸ Indeed, studies have demonstrated that EGF stimulates YAP activity in *Drosophila* and MCF-10A cells, which contributes to cell proliferation.^{19, 20} However, other studies have shown that EGF has no significant effect on YAP phosphorylation^{21, 22}. Therefore, the role of the EGFR signaling pathway on the regulation of YAP activity remains unclear. Whether the activation of EGFR family of tyrosine kinase receptors (ERBB) and the Hippo/YAP signaling pathway interact with each other to regulate ovarian cancer progression has not been investigated.

In the present study, we examine the relationship between YAP expression and the clinicopathological outcomes of ovarian cancer with large cohort of patient samples, and determine the role of YAP in the initiation and progression of ovarian cancer *in vitro* and *in vivo*. Our results show that the expression of YAP is associated with poor prognosis of ovarian cancer patients. Overexpression of YAP is sufficient to induce transformation of immortalized human ovarian surface epithelial cells (HOSE) and to initiate formation of ovarian tumors *in vivo*. Our mechanistic studies reveal the existence of an HBEGF & NRGs/

ERBB3/YAP/HBEGF & NRGs positive feedback loop, which may play a critical role in regulating the development and progression of ovarian cancer.

RESULTS

YAP expression is associated with poor prognosis in human ovarian cancer

To clarify the association between YAP expression and clinical outcomes of ovarian cancer patients, we quantified the expression of YAP in 42 normal human ovarian tissues and 342 ovarian cancer tissues by immunohistochemistry (IHC). The YAP immunosignal was low or undetectable in normal ovarian samples (Fig. 1a, 1d). In contrast, YAP levels were significantly increased in the tumor tissues, with higher level in advanced stage ovarian cancer samples (Fig. 1a–1d). Both positivity and intensity of the YAP immunosignals were associated with the progression of ovarian cancer (Fig. 1b& 1c). YAP immunostaining was primarily detected in the nucleus of cancer cells (Fig. 1d).

To determine whether YAP expression is associated with patient survival, overall survival data of patients with ovarian cancer were stratified into two groups (low & high) based on the intensity of YAP immunosignal. Kaplan-Meier survival estimation indicated that higher YAP levels were significantly associated with poor patient overall survival ($p = 0.018$) (Fig. 1e). Additionally, the positivity of YAP staining significantly correlated with the primary tumor (Fig. 1f), regional lymph nodes status (Fig. 1g), and tumor metastasis (Fig. 1h). Overall, YAP expression in serous, mucinous, clear cell, and endometrioid tumor tissues had no significant difference (supplementary Fig. S1a). If the data was normalized with stage, tumor type also had no correlation with YAP expression (supplementary Fig. S1b). YAP expression was not associated with tumor grade (supplementary Fig. S1c).

YAP promotes proliferation of normal and cancerous ovarian cells *in vitro*

We prepared six human cell lines with differential YAP levels and activities to determine the effect of YAP on the proliferation of normal and cancerous ovarian cells. HOSE-YAP^{S127A} and TOV21G-YAP^{S127A} cell lines express constitutively activated YAP1. HOSE-YAP and TOV21G-YAP overexpress wild-type YAP1. HOSE-MXIV and TOV21G-MXIV cells were transfected with empty vectors (MXIV) and used as controls. Western blot analysis showed that YAP was successfully overexpressed in HOSE-YAP, TOV21G-YAP, HOSE-YAP^{S127A} and TOV21G-YAP^{S127A} cells (Fig. 2a& 2b). YAP in HOSE-YAP^{S127A}, and TOV21G-YAP^{S127A} cells were constitutively activated, which is indicated by the low level of phosphorylated YAP (Fig. 2a& 2b). Consistent with Western blot results, HOSE-YAP, TOV21G-YAP, HOSE-YAP^{S127A}, and TOV21G-YAP^{S127A} cells continue to grow in complete medium (with 10% FBS) even after cells reached confluence; HOSE-YAP^{S127A} and TOV21G-YAP^{S127A} cells exhibited the highest growth rates, while cell growth in control groups slowed (TOV21G) or totally stopped after cells reached confluence (Fig. 2a& 2b). Consistent with these results, knockdown of YAP using YAP siRNA reduced TOV21G cell proliferation ($p < 0.001$) (Fig. 2c). We observed that FBS suppressed YAP phosphorylation in HOSE cells (Fig. 2d). In the FBS reduced culture medium, overexpression or constitutive activation of YAP significantly stimulated HOSE cell proliferation regardless of cell density ($p < 0.01$) (Fig. 2e).

In a 3D hanging drop culture system, HOSE-YAP^{S127A} cells formed the largest spheroids after incubation for 16 days, while the HOSE-MXIV cells formed the smallest spheroids. Similarly, Ki67 was localized to almost every cells in microtissues derived from HOSE-YAP^{S127A} cells, while it was localized to only few cells in microtissues derived from HOSE-MXIV cells (Fig. 3a). Verteporfin²³ not only suppressed cell proliferation (supplementary Fig. S2a), but also disrupted cell-cell communication, which was evidenced by the loose, incompletely formed spheroids and scattered distribution of cells in the culture (Fig. 3b). TUNEL assay showed that interrupting the interaction between YAP and TEAD by addition of verteporfin to the culture also significantly increased cell apoptosis (Fig. 3c, supplementary Fig. S2b).

YAP is able to transform normal ovarian cancer cells and enhance anchorage-independent cancer cell growth

The Soft Agar Assay was used to determine the tumorigenicity of YAP *in vitro*. HOSE-T80 (HOSE) cell is an immortalized non-tumorigenic cell line. HOSE-MXIV cells, like the parental HOSE cells, formed few or no colonies on the soft agar. The HOSE-YAP and HOSE-YAP^{S127A} cells formed many large colonies (Fig. 4a). In particular, the HOSE-YAP^{S127A} cells formed the majority of the colonies, indicating that colony formation was dependent on the presence of activated YAP (Fig. 4a). Quantitative analysis showed that overexpression or constitutive activation of YAP significantly stimulated anchorage-free growth of HOSE cells (MXIV vs YAP $p < 0.0001$; YAP vs YAP^{S127A} $p < 0.05$) (Fig. 4b). In the TOV21G ovarian cancer cell line-derived cells, TOV21G-YAP and TOV21G-YAP^{S127A} cells also formed significantly more colonies than from TOV21G-MXIV control cells (Fig. 4c& 4d, MXIV vs YAP $p < 0.0001$; YAP vs YAP^{S127A} $p < 0.001$).

YAP is sufficient to induce tumorigenesis and enhance tumor growth *in vivo*

To confirm the oncogenic role of YAP in ovarian cells *in vivo*, HOSE-MXIV, HOSE-YAP, and HOSE-YAP^{S127A} cells were injected subcutaneously into athymic nude mice. Overexpression or constitutive activation of YAP in HOSE cells was sufficient to induce tumorigenesis in 100% of the mice (ten out of ten) two weeks after cell injection (Fig. 5a). No tumors were observed in the HOSE-MXIV cell injected group. The tumors derived from HOSE-YAP^{S127A} cells grew faster than tumors derived from the HOSE-YAP cells (Fig. 5a).

To determine if YAP also enhanced cancer cell growth *in vivo*, TOV21G-MXIV, TOV21G-YAP, and TOV21G-YAP^{S127A} cells were also injected subcutaneously into athymic nude mice. As expected, all three cell lines formed tumors in the athymic mice. In comparison to the controls, tumors derived from TOV21G-YAP and TOV21G-YAP^{S127A} cells grew dramatically faster (Fig. 5b). The tumor size and weight in these two groups were significantly increased ($p < 0.001$; Fig. 5c). Immunofluorescent histochemistry analysis showed that YAP immunosignals in tumor tissues derived from TOV21G-YAP and TOV21G-YAP^{S127A} cells were stronger than in control tissues (derived from TOV21G-MXIV cells) (Fig. 5d). Moreover, the YAP immunosignal was primarily located to the nucleus of tumor cells (Fig. 5d). Consistent with these results, the Ki67 immunostaining in tumor tissues derived from TOV21G-YAP and TOV21G-YAP^{S127A} tumors was considerably

greater than staining present in tumors derived from the control cell line (TOV21G-MXIV) (Fig. 5e, supplementary Fig. S3).

YAP regulates expression of EGF-like ligands and ERBB receptors

Amphiregulin (AREG), an EGFR ligand, has been identified as a YAP target gene in breast epithelial cells.^{24, 25} However, overexpression of YAP did not affect *AREG* mRNA expression in HOSE, TOV21G and KGN cells (Fig. 6a, supplementary Fig. S4, Fig. S6). Instead, we found that YAP overexpression or activation drastically increased mRNA levels of two ERBB receptors, *EGFR* and *ERBB3*, and three ligands, heparin-binding EGF (*HBEGF*), Neuregulin-1 (*NRG1*) and Neuregulin-2 (*NRG2*) in these cell lines (Fig. 6a, supplementary Fig. S4-S7). Western blot analysis showed that overexpression or constitutive activation of YAP increased EGFR and ERBB3 protein levels in HOSE, KGN, and TOV21G cells (Fig. 6b, supplementary Fig. S8a). We also found that YAP knockdown successfully reduced the expression of EGFR, ERBB3, *HBEGF*, and *NRGs* in TOV21G cells (Fig. 6e & 6f) and KGN cells (supplementary Fig. S8b). Most importantly, overexpression or constitutive activation of YAP induced significant increase in the secretion of HBEGF and NRG1 in the culture medium (Fig. 6f & 6g, supplementary Fig. S9). Knockdown of YAP significantly reduced HBEGF and NRG1 concentrations in the culture medium (Fig. 6h & 6i).

To test whether YAP also regulated ERBB receptors and ligands *in vivo*, we used immunofluorescent histochemistry and/or RT-PCR to determine the expression of HBEGF, NRG1, NRG2, EGFR and ERBB3 expression in human tumors xenografts (derived from TOV21G-MXIV, TOV21G-YAP & TOV21G-YAP^{S127A}) in the athymic nude mice. The results showed that the protein levels of EGFR and ERBB3, and the mRNA levels of *HBEGF*, *NRG1*, *NRG2*, *EGFR*, and *ERBB3* were dramatically induced in tumor xenografts derived from TOV21G-YAP & TOV21G-YAP^{S127A} cells compared with that of the control group (from TOV21G-MXIV cells) (Fig. 6c & 6d).

We have also found that YAP regulates the expression of ERBB3 and the production of HBEGF and NRGs may depends on its interaction with transcription factor TEAD, because treatment of HOSE-MXIV, HOSE-YAP and HOSE-YAP^{S127A} cells with 5 μ M verteporfin, which inhibits the interaction between YAP and TEAD,²³ significantly blocked YAP-induced mRNA expression of *ERBB3*, *HBEGF*, *NRG1* and *NRG2* (supplementary Fig. S10). Most importantly, blocking the interaction of YAP and TEAD with verteporfin drastically reduced the production of free HBEGF in the both 2D and 3D culture system, and eliminated the secretion of NRG1 in both 2D and 3D culture system (Supplementary Fig. S10).

Interactions between YAP and ERBB pathways regulate ovarian cell proliferation

Because HBEGF specifically binds to EGFR and ERBB4, while NRG1 and NRG2 specifically bind to ERBB3 and ERBB4 to regulate cancer cell proliferation,²⁶ we designed experiments to determine whether these ligands and receptors are involved in YAP-mediated ovarian cancer cell growth. Treatment with recombinant human NRG1- β 1 and HBEGF significantly increased TOV21G and KGN cells proliferation (Fig. 7a & 7b). Moreover,

HBEGF and NRG1- β 1 also significantly stimulated proliferation of HOSE cell in a more physiological-relevant 3D hanging drop culture system (Fig. 7c& 7d).

Knockdown of HBEGF in HOSE and TOV21G cells with different YAP activity levels partially but significantly blocked YAP-induced cell proliferation (Fig. 7e& 7f, supplementary Fig. S11). However, knockdown of ERBB3 completely blocked YAP-induced proliferation of HOSE and TOV21G cells with different YAP activities (Fig. 7e & 7f, supplementary Fig. S11). These results suggest that the ERBB receptors and ligands contributed to YAP-mediated cell proliferation in both normal and cancerous ovarian cells.

In addition, knockdown of HBEGF or ERBB3 dramatically reversed oncogenic transformation in HOSE cells and inhibited YAP-induced enhancement of anchorage-independent growth of TOV21G cells, as indicated by a significant decrease in the colony formation induced by YAP overexpression or constitutive activation ($p < 0.0001$) (Fig. 8a-8d), indicating that ERBB3 and HBEGF contribute to YAP-mediated anchorage-independent cell growth.

The interaction between the Hippo/YAP and the ERBB signaling pathways is required for HBEGF and NRG1 stimulation of ovarian cancer cell growth

In confluent TOV21G ovarian cancer cells, YAP was highly phosphorylated following serum starvation. Treatment of confluent TOV21G cancer cells with HBEGF and NRG1 β 1 resulted in a rapid and significant decrease in phosphorylation of LATS1, MOB1 and YAP (Fig. 9a, supplementary Fig. S12). This evidence indicates that the Hippo pathway may be involved in mediation of the HBEGF- and NRG1-activated ERBB signals in the ovarian cancer cells, because LATS1 and MOB1 are main components of the Hippo/YAP pathway. HBEGF and NRG1 β 1 also induced rapid phosphorylation of ERBB receptors and activation of the PI3K and MAPK pathways in TOV21G cells (supplementary Fig. S13, Fig. S14). Blockade of EGFR (with AG1478), PI3K (with LY294002), or MEK1/2 (with UO126) eliminates HBEGF- and NRG1-induced dephosphorylation of YAP (supplementary Fig. S15), suggesting the involvement of PI3k and MAPK signaling pathway in the interaction between the Hippo/YAP and the ERBB pathways in the ovarian cancer cells. The involvement of PI3K pathway is further evidenced by the observation that pretreatment of HOSE-YAP and HOSE-YAP^{S127A} cells with LY294002 (PI3K inhibitor) or verteporfin (YAP antagonist) totally blocked their ability to form colonies in the soft agar (supplementary Fig. S16). MAPK may only partially involved in the YAP-induced transformation of ovarian surface epithelial cells because UO126 only partially blocked YAP-induced colony formation in HOSE-YAP and HOSE-YAP^{S127A} cells (supplementary Fig. S16).

Knockdown of HBEGF or ERBB3 blocked YAP-induced formation of spheroids by HOSE cells and suppressed the growth of HOSE cells in the 3D culture system (Fig. 9b). Knockdown of YAP not only eliminated HBEGF- and NRG1 β 1-induced TOV21G cell proliferation, but also suppressed the basal proliferation of TOV21G. (Fig. 9c). Similar results were observed in KGN cells (Fig. 9d). Intriguingly, treatment of confluent TOV21G cells with HBEGF and NRG1 β 1 for 48 hours stimulated the transcription of *ERBB3*, *HBEGF*, *NRG1*, and *NRG2* genes (Supplementary Fig. S17).

DISCUSSION

YAP has been identified as the essential downstream effector of Hippo pathway. YAP is frequently up regulated in a wide spectrum of human solid tumors and significantly associated with poor clinical outcomes.^{10, 27-29} In ovarian cancer, the relationship between YAP expression and clinical outcomes is somewhat controversial. Hall *et al.* reported that high levels of nuclear YAP, or low levels of cytoplasmic phosphorylated YAP, is associated with poor survival of ovarian cancer patients.^{9, 30} However, Zhang *et al.* did not observed any association between YAP expression and clinical outcomes in serous cancers. In their study, correlation between nuclear YAP and poor survival is limited to patients with ovarian clear cell carcinoma.¹⁰ The discrepancy can be attributed to the relatively small sample size in these studies. In the present study, using large cohort of patient samples, we found that total YAP staining strongly correlated with stage and TNM status (tumor, lymph node, and metastasis staging) was significantly associated with poor patient survival. Further analysis showed that total YAP staining was strongly correlated with stage and TNM status. Our results are consistent with previous reports in multiple human cancers,^{28, 31, 32} and indicate that YAP activity may play a causal role on ovarian cancer progression and metastasis. Nevertheless, we realize the limitation of IHC-based detection and analysis systems. The utility of YAP as an independent prognostic marker of ovarian cancer needs to be extensively verified using additional approaches.

Human ovarian cancer has been traditionally thought to originate from human ovarian surface epithelial cells (HOSE);³³ although recent studies indicate that fallopian tube epithelial cells might also be an origin for serious ovarian epithelial cancer.³⁴ How these epithelial cells are transformed into tumorigenic cells *in vivo* and what drives the early stage expansion and progressions of the initial tumor(s) under physiological conditions are open questions. Transfection of HOSE cells with SV40T/t and HPV16 E6/E7 extended the life span of these cells, but the transfected cells were not tumorigenic.³⁵ Disruption of TP53 and RB1 pathway by SV40 early genomic region and hTERT immortalized but did not transform human OSE.³⁶ Introduction of *HRAS*^{V12} or *KRAS*^{V12} into the immortalized cells, however, allowed them to form subcutaneous tumors after injection into immunocompromised mice.³⁶ In the present study, we found that overexpression of wild type YAP or constitutively active YAP was sufficient for transformation of immortalized normal human ovarian surface epithelial cells. Our study also indicated that overexpression of wild type YAP or constitutively active YAP promoted cancerous ovarian epithelial cell growth both *in vivo* and *in vitro*, consistent with previous *in vitro* studies showing that YAP acts as an ovarian oncogene.^{3, 9, 36} Hall et al showed that overexpression of YAP^{5SA} (in which all five serine phosphorylation sites in YAP gene were mutated to alanine) was able to induce the colony formation in ovarian surface epithelial cells.⁹ Our present study is the first direct *in vivo* evidence showing that overexpression of YAP in human ovarian surface epithelial cells is sufficient to initiate tumors. Our study clearly shows that overexpression of YAP is a potential event for initiation and progression of ovarian cancer. Since HOSE-T80 cells are immortalized with SV40T/t and hTERT,³⁶ we cannot exclude a synergetic effect of YAP with the viral genes on the tumorigenicity of HOSE cells. Recently, Sasaki *et al.* established an immortalized HOSE cells by expressing mutant Cdk4, cyclin D1 and hTERT.³⁷ Since this

human OSE cell line was immortalized without involvement of virus, it may be a valuable tool for studying the role of YAP in the transformation of human OSE.

The mechanism underlying YAP regulation of initiation and progression of ovarian cancer is unclear. One recent report suggested that YAP-stimulated production of AREG in ovarian cancer cells can regulate ovarian cancer progression.³ However, other investigators showed that overexpression or activation of YAP had no effect on AREG expression.^{7, 14} Similarly, we found that AREG expression was not affected by overexpression or activation of YAP in HOSE-T80, TOV21G, and KGN cells. However, we did find a significant increase in AREG expression in cervical cancer cells after YAP overexpression [He & Wang, unpublished data]. By examining the mRNA expression profile of all EGF-like ligands and ERBBs in our YAP activity modified cell lines, we found that expression of *HBEGF*, *NRG1* and *NRG2* was consistently up-regulated by YAP in HOSE and ovarian cancer cell lines (Fig. 6, supplementary Fig. S4-S7). It is known that HBEGF signals through EGFR and ERBB4, while NRG1 signals through ERBB3 and ERBB4. Although interaction between YAP and ERBB4 has been reported previously,^{38, 39} our results show that in the receptor level, only EGFR and ERBB3 are consistently up-regulated by YAP overexpression or constitutive activation in the ovarian cells. ERBB2 level was not significantly changed by YAP expression or activation, while ERBB4 is regulated by YAP protein in a cell type-dependent manner. Therefore, in the ovarian cancer cells, the Hippo/YAP signaling pathway may interact with the ERBB signaling pathway, especially the HBEGF- and neuregulin-activated EGFR and ERBB3 signaling pathways, to drive the initiation and progression of ovarian cancer. However, a potential interaction between YAP and ErbB4, which has been reported in other cancer cell types^{38, 39}, may also exist in the ovarian cancer cells and deserves further investigations.

Expressions of EGFR, ERBB3, HBEGF, NRG1 and NRG2 have been implicated in both normal organ development and malignancy.²⁶ The expression and function of EGFR and ERBB2 in breast and ovarian cancer have been extensively studied. However, roles of ERBB3 in ovarian cancer initiation and progression are not well defined. A recent study showed that in a portion (~25%) of ovarian cancers, NRG1 activated ERBB3 to promote cancer cell proliferation and drive tumor growth.⁴⁰ Consistent with this finding, in the present study, we found that NRG1 was able to promote TOV21G and KGN cell proliferation (Fig. 7a& 7b). Interestingly, we found that overexpression of YAP or constitutively active YAP in TOV21G or KGN ovarian tumor cells dramatically induced NRG1 production and ERBB3 expression. Knockdown of ERBB3 eliminated the stimulatory effect of YAP on cancer cell proliferation (Fig. 7e& 7f), and nearly abrogated YAP-enhanced anchorage-independent growth of TOV21G cells. These results clearly indicate that YAP has the potential to control ovarian cancer cell proliferation via regulating the NRG1/ERBB3 pathway. Intriguingly, we found that NRG1 was able to rapidly suppress Hippo pathway and activate YAP by dephosphorylating LATS1, MOB1 and YAP (Fig. 9). Simultaneously, NRG1 also stimulated the expression of *ERBB3*, *NRG1*, *NRG2*, and *HBEGF*. Knockdown of YAP in ovarian cancer cells suppressed the basal growth in these cells and eliminated NRG1-stimulated cancer cell proliferation (Fig. 9). Taken together, our data indicate the existence of an NRG1/ERBB3/YAP/NRG1 autocrine loop in the ovarian

cancer cells. This autocrine loop appears to play a critical role in the initiation and progression of ovarian cancers.

HBEGF has been shown to play a critical role in the ovarian tumorigenesis and tumor progression.⁴¹ In the present study, we found that overexpression or constitutive activation of YAP also increased production of free HBEGF and expression of EGFR (the selective receptor for HBEGF). Knockdown of YAP in cancer cells suppressed production of free HBEGF and expression of *EGFR*. Like NRG1, HBEGF also stimulated ovarian cancer cell growth. Moreover, HBEGF was able to suppress phosphorylation of LATS1, MOB1 and YAP and stimulate production of NRG1 and free HBEGF, and expression of *ERBB3*. These results suggest the potential presence of a pro-proliferation HBEGF/EGFR/YAP/HBEGF autocrine loop in the ovarian cancer cells. A recent report indicates that the EGFR-RAS-MAPK signaling promotes phosphorylation of the Ajuba family protein WTIP and thus enhances WTIP binding to LATS and WW45, leading to suppression of Hippo pathway and activation of YAP²⁰. This evidence strongly supports our findings. Interestingly, we found that treatment of TOV21G with HBEGF within 2 hours, but not NRG1, nearly eliminated the expression of EGFR receptor (supplementary Fig. S13 & Fig. S14). This observation is consistent with previous finding that HBEGF binding lead to the rapid lysosomal degradation of EGFR.⁴² Therefore, HBEGF and neuregulin may regulate ovarian cancer progression in different ways: neuregulin constitutively stimulates ovarian cancer progression through a positive autocrine/paracrine loop, while HBEGF may amplify the NRG1/ERBB3/YAP/NGR1 autocrine loop.

YAP has been showed to act mainly through its direct interaction with TEAD/TEF family to regulate downstream genes expression.^{5, 6} Verteporfin is a selective antagonist of YAP functioning by interrupting YAP-TEAD interaction.²³ Our data show that verteporfin not only inhibits YAP-induced transformation of ovarian surface epithelial cells, suppressed YAP-enhanced growth of normal and ovarian cancer cells, but also blocked YAP-induced production of free HBEGF and NRG1, as well as expression of ERBB3 receptor. Clearly, YAP regulation of the initiation and progression of ovarian cancer may depend on its proper interaction with the TEAD transcription factor. Recent studies showed that beside TEAD, YAP also interacts with others transcriptional factors, such as Smad, Runx1/2, p73, Pax3, and TBX5 (a list that is still rapid growing), to regulate downstream gene expression.^{5, 6} These transcription factors may also be important for the ovarian cancer initiation and progression and need further studies.

In conclusion, our present study shows that YAP has the potential to transform the ovarian surface epithelial cells, leading to initiation and progression of ovarian cancer. YAP (potentially in a Hippo pathway dependent manner) forms autocrine loops with the ERBB signaling pathway to induced the initiation and promote the progression of ovarian cancer (Fig. 10). Although up regulation of EGFR, ERBB2, and ERBB3 is found in 60%, 18%, and 50% of epithelial ovarian cancer tissues, respectively, the clinical trial results with single agent EGFR inhibitors such as erlotinib, gefitinib, trastuzumab or pertuzumab, have proven to be of little benefit in randomized trials.⁴³ The identification of a NRG1/ERBB3/YAP/NGR1 autocrine loop in ovarian cancers suggests that ERBB3 will be a promising target for ovarian cancer. MM-121, a monoclonal ERBB3-directed antibody, is currently under

investigation in phase II trials. Combined targeting the Hippo/YAP pathway and ERBB pathways, especially the NRG1/ERBB3 pathway, has potential to provide a novel therapeutic strategy for ovarian cancer treatment.

MATERIALS AND METHODS

Chemicals

HBEGF and NRG1 β 1 were from R&D Systems Inc. (Minneapolis, MN). Cell culture medium was from Sigma-Aldrich (St. Louis, MO). FBS was from Atlanta Biologicals, Inc. (Lawrenceville, GA). Ribogreen RNA quantification kit and Alexa-conjugated secondary antibodies were from Life TechnologiesTM (Grand Island, NY). YAP siRNAs were from Dharmacon/Thermo Scientific (Pittsburgh, PA), HBEGF and ERBB3 siRNA were from Santa Cruz Biotechnology, Inc. (Dallas, Texas) and Life TechnologiesTM (supplementary Fig. S18). Antibodies against total and phosphorylated YAP, LATS1, MOB1, ErbBs, ATK and ER1/2 were from Cell Signaling Technology Inc. (Danvers, MA).

Cell Lines and Human Ovarian Tissues

TOV21G, an ovarian epithelial cancer cell line, was purchased from ATCC (Manassas, VA). KGN, an ovarian granulosa cell tumor cell line, was obtained from the Riken Biosource Center (Riken Cell Bank, Ibaraki, Japan). Immortalized human normal ovarian epithelial cells (HOSE-T80) were from Dr. Bo R Reuda at Massachusetts General Hospital (Boston, MA). Human ovarian tissue microarray slides were purchased from Biomax (Rockville, MD).

Immunohistochemistry

YAP expression in ovarian tissues was detected using a peroxidase-based immunohistochemistry, the immunosignal was visualized with DAB kit (Invitrogen, Carlsbad, CA). Sections were scanned with an iSCAN Coreo Slide Scanner (Ventana Medical Systems, Inc., Oro Valley, AZ, USA). The intensity of the positive signal was quantified using Aperio ImageScope software (Aperio[®] Technologies, Inc., Vista, CA).

Cell Transfection

Nine cell lines were established to determine the effect of YAP on ovarian cancer cell proliferation. Briefly, HOSE80, TOV21G, and KGN cells were cultured to 40% confluent and then transfected with retrovirus-based YAP overexpression constructs (YAP, YAP^{S127A}) or empty vector (MXIV). Stable transfected clones were selected using G418. Cell growth was determined by counting the cell number using an Invitrogen Countess[®] Automated cell counter (Invitrogen Corporation, Carlsbad, CA).

Three-dimension hanging drop cell culture and Colony Formation Assays

Two three-dimension (3D) hanging drop culture systems were used to examine the role of YAP in the cell proliferation and cell-cell communication. Briefly, Cells (0.5×10^6) were cultured in Perfecta3D (3D Biomatrix, Ann Arbor, MI) or GravityPLUSTM 3D Cell Culture plates (InSphero, Schlieren, Switzerland) according to the company's instruction. Cytoselect

96-Well Cell Transformation assay kit (Cell Biolabs, Inc., San Diego, CA) was used to determine the effect of YAP on the anchorage-independent growth of ovarian cells.

RT-PCR and Western Blot Analysis

Total RNA was prepared by RNeasy Mini Kit (QIAGEN, Valencia, CA), and reverse transcription was completed by using SuperScript First-Strand kit (Life Technology™, Grand Island, NY). RT-PCR was run on MJ PTC100 Programmable Thermal cycler (Bio-Rad Laboratories, Hercules, CA) with a protocol established in our laboratory.^{44, 45} The primers have been validated previously.⁴⁶ Protein levels were determined with Western Blot with a protocol established in our laboratory.^{44, 45} The immunosignal was detected by using The SuperSignal West Femto Chemiluminescent Substrate Kit (Pierce/Thermo Scientific, Rockford, IL); the images were captured and analyzed with a UVP gel documentation system (UVP, LLC, Upland, CA).

In Vivo Tumorigenicity

5×10^6 cells / 0.1 mL PBS were injected subcutaneously into the dorsal flank of 7-week-old female athymic nude mice (n=5). Tumor volume (mm^3) was calculated as follows: volume = (shortest diameter)² x (longest diameter) X 3.14 ÷ 6. The animal handling procedures and all experimental protocols were approved by the Institutional Animal Care and Use Committee (IACUC) at the University of Nebraska Medical Center.

Immunofluorescent Histochemistry (IF)

Frozen sections at 6 μm were stained with a protocol established in our laboratory.^{44, 45} Images were captured using a Zeiss 710 Meta Confocal Laser Scanning Microscope and analyzed using the Zeiss Zen 2010 software (Carl Zeiss Microscopy, LLC, Thornwood, NY). TUNEL assay was performed using TUNEL Apoptosis Detection kit (EMD Millipore, inc. Darmstadt, Germany) to determine cell apoptosis.

Statistical Analysis

All experiments were repeated at least three times unless otherwise noted. Statistical analyses were conducted primarily using GraphPad Prism software (GraphPad Software, Inc.). Data were analyzed for significance by one-way ANOVA with Tukey's post-Hoc test. A value of $p < 0.05$ was considered to be significant.

Supplementary Material

Refer to Web version on PubMed Central for supplementary material.

Acknowledgments

This work was supported by the Eunice Kennedy Shriver National Institute of Child Health and Human Development (5R00HD059985, 5P01AG029531); The Olson Center for Women's Health (no number); The Fred & Pamela Buffett Cancer Center (LB595); the Omaha Veterans Administration Medical Center (5101BX000512) and The National Institute of Food and Agriculture (2011-67015-20076). We wish to thank for Melody A. Montgomery at the University of Nebraska Medical Center Research Editorial Office for her professional assistance in editing this manuscript.

References

1. Siegel R, Desantis C, Jemal A. Colorectal cancer statistics, 2014. *CA Cancer J Clin.* 2014; 64:104–117. [PubMed: 24639052]
2. Bast RC Jr, Hennessy B, Mills GB. The biology of ovarian cancer: new opportunities for translation. *Nat Rev Cancer.* 2009; 9:415–428. [PubMed: 19461667]
3. Justice RW, Zilian O, Woods DF, Noll M, Bryant PJ. The *Drosophila* tumor suppressor gene *warts* encodes a homolog of human myotonic dystrophy kinase and is required for the control of cell shape and proliferation. *Genes Dev.* 1995; 9:534–546. [PubMed: 7698644]
4. Xu T, Wang W, Zhang S, Stewart RA, Yu W. Identifying tumor suppressors in genetic mosaics: the *Drosophila* *lats* gene encodes a putative protein kinase. *Development.* 1995; 121:1053–1063. [PubMed: 7743921]
5. Pan D. The hippo signaling pathway in development and cancer. *Dev Cell.* 2010; 19:491–505. [PubMed: 20951342]
6. Yu FX, Guan KL. The Hippo pathway: regulators and regulations. *Genes Dev.* 2013; 27:355–371. [PubMed: 23431053]
7. Dong J, Feldmann G, Huang J, Wu S, Zhang N, Comerford SA, et al. Elucidation of a universal size-control mechanism in *Drosophila* and mammals. *Cell.* 2007; 130:1120–1133. [PubMed: 17889654]
8. Lee KP, Lee JH, Kim TS, Kim TH, Park HD, Byun JS, et al. The Hippo-Salvador pathway restrains hepatic oval cell proliferation, liver size, and liver tumorigenesis. *Proc Natl Acad Sci U S A.* 2010; 107:8248–8253. [PubMed: 20404163]
9. Hall CA, Wang R, Miao J, Oliva E, Shen X, Wheeler T, et al. Hippo pathway effector Yap is an ovarian cancer oncogene. *Cancer Res.* 2010; 70:8517–8525. [PubMed: 20947521]
10. Zhang X, George J, Deb S, Degoutin JL, Takano EA, Fox SB, et al. The Hippo pathway transcriptional co-activator, YAP, is an ovarian cancer oncogene. *Oncogene.* 2011; 30:2810–2822. [PubMed: 21317925]
11. Harvey KF, Zhang X, Thomas DM. The Hippo pathway and human cancer. *Nat Rev Cancer.* 2013; 13:246–257. [PubMed: 23467301]
12. Yuan M, Tomlinson V, Lara R, Holliday D, Chelala C, Harada T, et al. Yes-associated protein (YAP) functions as a tumor suppressor in breast. *Cell Death Differ.* 2008; 15:1752–1759.
13. Strano S, Monti O, Pediconi N, Baccarini A, Fontemaggi G, Lapi E, et al. The transcriptional coactivator Yes-associated protein drives p73 gene-target specificity in response to DNA Damage. *Mol Cell.* 2005; 18:447–459. [PubMed: 15893728]
14. Cai H, Xu Y. The role of LPA and YAP signaling in long-term migration of human ovarian cancer cells. *Cell Commun Signal.* 2013; 11:31. [PubMed: 23618389]
15. Lucas EP, Khanal I, Gaspar P, Fletcher GC, Polesello C, Tapon N, et al. The Hippo pathway polarizes the actin cytoskeleton during collective migration of *Drosophila* border cells. *J Cell Biol.* 2013; 201:875–885. [PubMed: 23733343]
16. Kojic N, Chung E, Kho AT, Park JA, Huang A, So PT, et al. An EGFR autocrine loop encodes a slow-reacting but dominant mode of mechanotransduction in a polarized epithelium. *FASEB J.* 2010; 24:1604–1615. [PubMed: 20056713]
17. Tschumperlin DJ. EGFR autocrine signaling in a compliant interstitial space: mechanotransduction from the outside in. *Cell Cycle.* 2004; 3:996–997. [PubMed: 15254423]
18. Curto M, Cole BK, Lallemand D, Liu CH, McClatchey AI. Contact-dependent inhibition of EGFR signaling by Nf2/Merlin. *J Cell Biol.* 2007; 177:893–903. [PubMed: 17548515]
19. Fan R, Kim NG, Gumbiner BM. Regulation of Hippo pathway by mitogenic growth factors via phosphoinositide 3-kinase and phosphoinositide-dependent kinase-1. *Proc Natl Acad Sci U S A.* 2013; 110:2569–2574. [PubMed: 23359693]
20. Reddy BV, Irvine KD. Regulation of Hippo signaling by EGFR-MAPK signaling through Ajuba family proteins. *Dev Cell.* 2013; 24:459–471. [PubMed: 23484853]
21. Yu FX, Zhao B, Panupinhu N, Jewell JL, Lian I, Wang LH, et al. Regulation of the Hippo-YAP pathway by G-protein-coupled receptor signaling. *Cell.* 2012; 150:780–791. [PubMed: 22863277]

22. Zhao B, Wei X, Li W, Udan RS, Yang Q, Kim J, et al. Inactivation of YAP oncoprotein by the Hippo pathway is involved in cell contact inhibition and tissue growth control. *Genes Dev.* 2007; 21:2747–2761. [PubMed: 17974916]
23. Liu-Chittenden Y, Huang B, Shim JS, Chen Q, Lee SJ, Anders RA, et al. Genetic and pharmacological disruption of the TEAD-YAP complex suppresses the oncogenic activity of YAP. *Genes Dev.* 2012; 26:1300–1305. [PubMed: 22677547]
24. Yang N, Morrison CD, Liu P, Miecznikowski J, Bshara W, Han S, et al. TAZ induces growth factor-independent proliferation through activation of EGFR ligand amphiregulin. *Cell Cycle.* 2012; 11:2922–2930. [PubMed: 22825057]
25. Zhang J, Ji JY, Yu M, Overholtzer M, Smolen GA, Wang R, et al. YAP-dependent induction of amphiregulin identifies a non-cell-autonomous component of the Hippo pathway. *Nat Cell Biol.* 2009; 11:1444–1450. [PubMed: 19935651]
26. Hynes NE, Lane HA. ERBB receptors and cancer: the complexity of targeted inhibitors. *Nat Rev Cancer.* 2005; 5:341–354. [PubMed: 15864276]
27. Steinhardt AA, Gayyed MF, Klein AP, Dong J, Maitra A, Pan D, et al. Expression of Yes-associated protein in common solid tumors. *Hum Pathol.* 2008; 39:1582–1589. [PubMed: 18703216]
28. Wang Y, Dong Q, Zhang Q, Li Z, Wang E, Qiu X. Overexpression of yes-associated protein contributes to progression and poor prognosis of non-small-cell lung cancer. *Cancer Sci.* 2010; 101:1279–1285. [PubMed: 20219076]
29. Xu MZ, Yao TJ, Lee NP, Ng IO, Chan YT, Zender L, et al. Yes-associated protein is an independent prognostic marker in hepatocellular carcinoma. *Cancer.* 2009; 115:4576–4585. [PubMed: 19551889]
30. Xia Y, Chang T, Wang Y, Liu Y, Li W, Li M, et al. YAP promotes ovarian cancer cell tumorigenesis and is indicative of a poor prognosis for ovarian cancer patients. *PloS One.* 2014; 9:e91770. [PubMed: 24622501]
31. Lamar JM, Stern P, Liu H, Schindler JW, Jiang ZG, Hynes RO. The Hippo pathway target, YAP, promotes metastasis through its TEAD-interaction domain. *Proc Natl Acad Sci U S A.* 2012; 109:E2441–2450. [PubMed: 22891335]
32. Kim JM, Kang DW, Long LZ, Huang SM, Yeo MK, Yi ES, et al. Differential expression of Yes-associated protein is correlated with expression of cell cycle markers and pathologic TNM staging in non-small-cell lung carcinoma. *Hum Pathol.* 2011; 42:315–323. [PubMed: 21190720]
33. Auersperg N, Wong AS, Choi KC, Kang SK, Leung PC. Ovarian surface epithelium: biology, endocrinology, and pathology. *Endocr Rev.* 2001; 22:255–288. [PubMed: 11294827]
34. Orsulic S, Li Y, Soslow RA, Vitale-Cross LA, Gutkind JS, Varmus HE. Induction of ovarian cancer by defined multiple genetic changes in a mouse model system. *Cancer Cell.* 2002; 1:53–62. [PubMed: 12086888]
35. Gregoire L, Rabah R, Schmelz EM, Munkarah A, Roberts PC, Lancaster WD. Spontaneous malignant transformation of human ovarian surface epithelial cells in vitro. *Clin Cancer Res.* 2001; 7:4280–4287. [PubMed: 11751530]
36. Liu J, Yang G, Thompson-Lanza JA, Glassman A, Hayes K, Patterson A, et al. A genetically defined model for human ovarian cancer. *Cancer Res.* 2004; 64:1655–1663. [PubMed: 14996724]
37. Sasaki R, Narisawa-Saito M, Yugawa T, Fujita M, Tashiro H, Katabuchi H, et al. Oncogenic transformation of human ovarian surface epithelial cells with defined cellular oncogenes. *Carcinogenesis.* 2009; 30:423–431. [PubMed: 19126650]
38. Omerovic J, Puggioni EM, Napoletano S, Visco V, Fraioli R, Frati L, et al. Ligand-regulated association of ErbB-4 to the transcriptional co-activator YAP65 controls transcription at the nuclear level. *Exp Cell Res.* 2004; 294:469–479. [PubMed: 15023535]
39. Komuro A, Nagai M, Navin NE, Sudol M. WW domain-containing protein YAP associates with ErbB-4 and acts as a co-transcriptional activator for the carboxyl-terminal fragment of ErbB-4 that translocates to the nucleus. *J Biol Chem.* 2003; 278:33334–33341. [PubMed: 12807903]
40. Sheng Q, Liu X, Fleming E, Yuan K, Piao H, Chen J, et al. An activated ErbB3/NRG1 autocrine loop supports in vivo proliferation in ovarian cancer cells. *Cancer Cell.* 2010; 17:298–310. [PubMed: 20227043]

41. Miyamoto S, Hirata M, Yamazaki A, Kageyama T, Hasuwa H, Mizushima H, et al. Heparin-binding EGF-like growth factor is a promising target for ovarian cancer therapy. *Cancer Res.* 2004; 64:5720–5727. [PubMed: 15313912]
42. Roepstorff K, Grandal MV, Henriksen L, Knudsen SL, Lerdrup M, Grovdal L, et al. Differential effects of EGFR ligands on endocytic sorting of the receptor. *Traffic.* 2009; 10:1115–1127. [PubMed: 19531065]
43. Banerjee S, Kaye SB. New strategies in the treatment of ovarian cancer: current clinical perspectives and future potential. *Clin Cancer Res.* 2013; 19:961–968. [PubMed: 23307860]
44. Wang C, Roy SK. Expression of E-cadherin and N-cadherin in perinatal hamster ovary: possible involvement in primordial follicle formation and regulation by follicle-stimulating hormone. *Endocrinology.* 2010; 151:2319–2330. [PubMed: 20219978]
45. Fu D, Lv X, Hua G, He C, Dong J, Lele SM, et al. YAP regulates cell proliferation, migration, and steroidogenesis in adult granulosa cell tumors. *Endocr-Relat Cancer.* 2014; 21:297–310. [PubMed: 24389730]
46. Amsellem-Ouazana D, Bieche I, Tozlu S, Botto H, Debre B, Lidereau R. Gene expression profiling of ERBB receptors and ligands in human transitional cell carcinoma of the bladder. *J Urology.* 2006; 175:1127–1132.

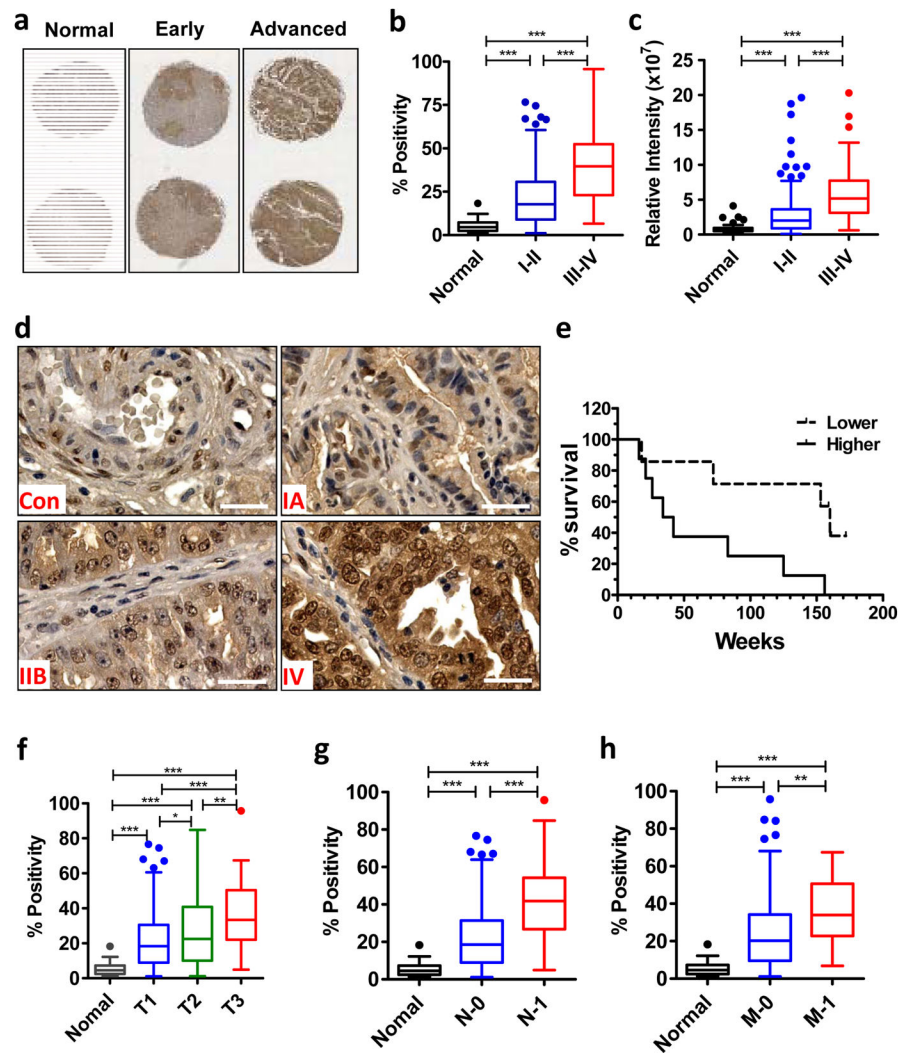


Fig. 1. Immunohistochemical analysis of YAP expression in ovarian tumor tissues
a) Representative images showed YAP protein distribution in tissues from age matched normal ovaries, early stage tumors and advanced stage tumors. **b)** Quantitative data showing the relationship of YAP positivity and tumor stages. **c)** Quantitative data showing the relationship of YAP relative intensity and tumor stages. **d)** Representative high-resolution images showing the subcellular distribution of YAP protein in the ovarian cancer tissues. Con: normal control; IA, IIB and IV: tumor stage IA, IIB, and IV; Scale bar: 40 μ m. **e)** Correlation between progression free survival and YAP protein expression in patient tissues. The patient samples with survival data were stratified in two groups based on the intensity of YAP immunostaining. **f, g & h)** Relationship between YAP staining positivity and primary tumor size (**f**), involvement of lymph node (**g**) and tumor metastasis status (**h**). Positivity: the number of YAP positive cells relative to the total cell number. For all bar graphs, each bar represents mean \pm SEM (see n values in table 1). Bars with different letters are significantly different from each other ($p < 0.05$).

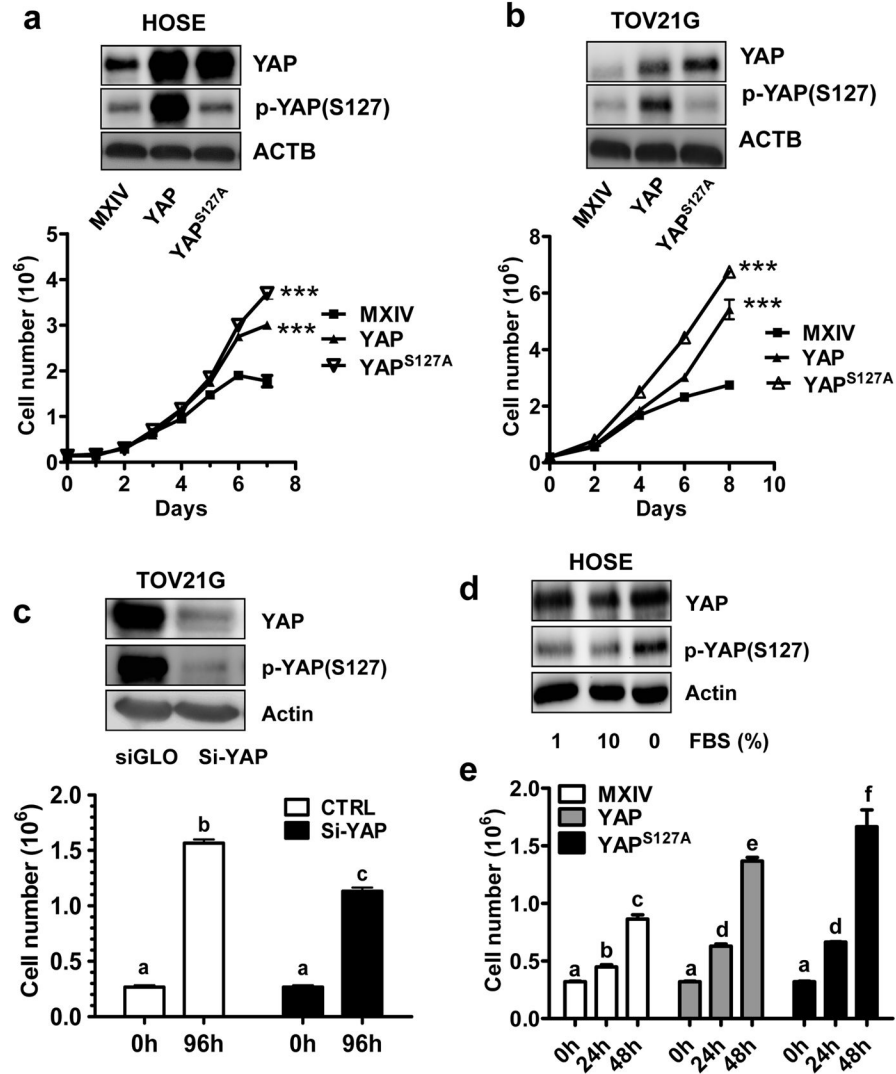


Fig. 2. YAP promotes proliferation in normal and cancerous ovarian cells

a) Top panel: Western blot detection of YAP and phosphorylated YAP levels in HOSE-MXIV, HOSE-YAP and HOSE-YAP^{S127A} cells. Lower panel: Growth curve of HOSE-MXIV, HOSE-YAP and HOSE-YAP^{S127A} cells cultured in medium in the presence of 10% FBS. **b)** Top panel: Western blot detection of YAP and phosphorylated YAP levels in TOV21G-MXIV, TOV21G -YAP and TOV21G -YAP^{S127A} cells; Lower panel: Growth curve of TOV21G -MXIV, TOV21G -YAP and TOV21G -YAP^{S127A} cells cultured in medium in the presence of 10% FBS. **c)** Top panel: Western blot detection of YAP protein before and after knockdown of YAP in TOV21G cells. YAP siRNA (si-YAP) successfully knocked down YAP protein. Lower panel, change of cell growth after knockdown of YAP in TOV21G cells. **d)** Western blot showing the effect of FBS on the expression and phosphorylation of YAP protein in HOSE cells. **e)** Growth of HOSE cell lines with different levels and activities of YAP in serum reduced culture medium (1% FBS). For all representative graphs, each point or bar represents mean ± SEM of 4 repeats. Bars with

different letters are significantly different from each other. ***: $p < 0.001$ compared with control group (MXIV).

Author Manuscript

Author Manuscript

Author Manuscript

Author Manuscript

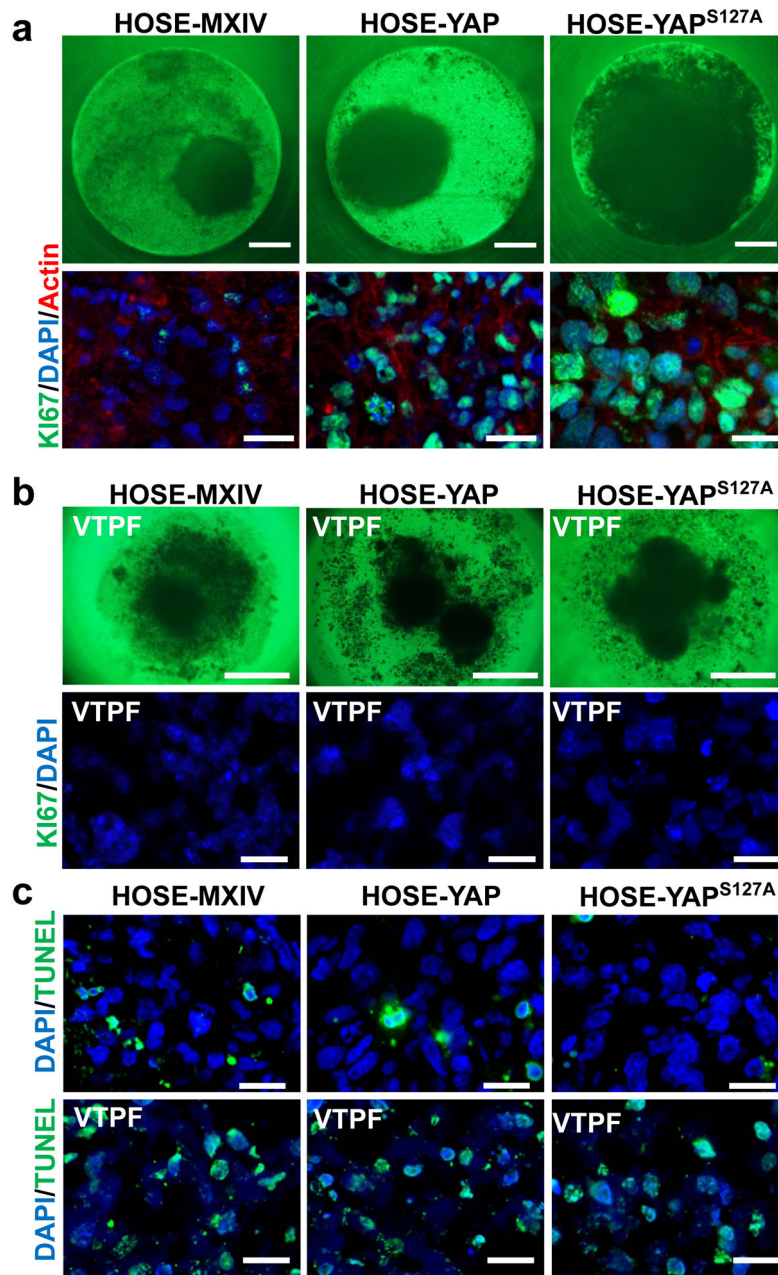


Fig. 3. YAP promotes cell growth and cell-cell communication in a 3D hanging drop culture system

a) Top panel: Representative images showing the spheroids derived from HOSE-MXIV, HOSE-YAP and HOSE-YAP^{S127A} cells growing in a 3D hanging drop culture system for 16 days. Lower panel: Ki67 staining (green) showing the differential proliferation of three cell lines in the spheroids. Nuclei were stained with DAPI (blue). Actin filaments were stained with rhodamin-phalloidin (red). Scale bar: 20 μ m. **b)** Top panel: Representative images showing the spheroids derived from HOSE-MXIV, HOSE-YAP and HOSE-YAP^{S127A} cells growing in 3D-culture system for 16 days in the presence of verteporfin (VTPF, 5 μ M, YAP antagonist). Lower panel: Ki67 staining (green) showing the proliferation of three cell lines

in the spheroids treated with 5 μ M verteporfin (VTPF). Nuclei were stained with DAPI (blue). Scale bar: 20 μ m. C) TUNEL assay to examine the apoptosis of cells in the spheroids derived from HOSE cell lines in the presence or absence of 5 μ M verteporfin (VTPF). Apoptotic cells were labeled with green color. Nuclei were stained with DAPI. Scale bar: 20 μ m.

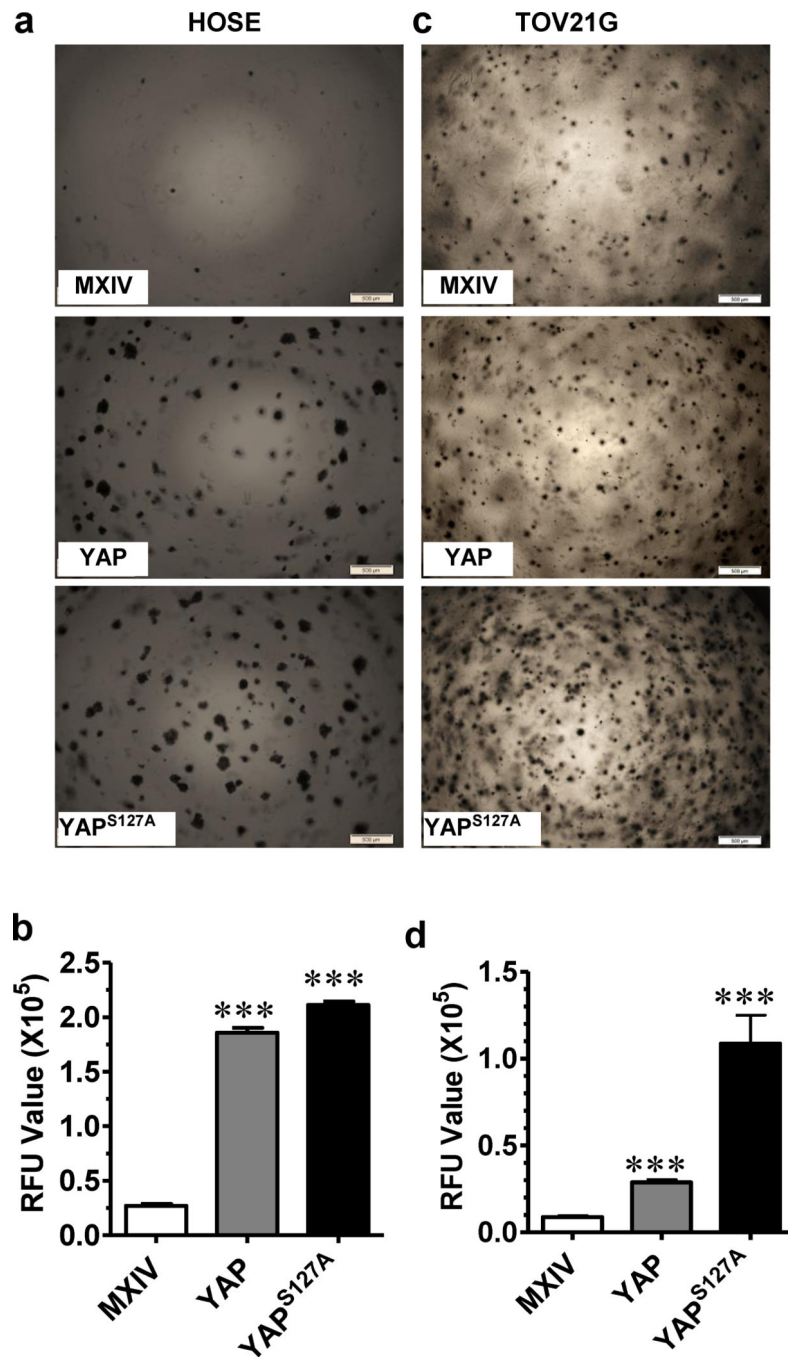


Fig. 4. Overexpression of wild type YAP or constitutively active YAP transformed human ovarian surface epithelial cells and enhanced anchorage-independent growth of ovarian cancer cells
a) Soft agar assay showing colony formation in HOSE-MXIV, HOSE-YAP and HOSE-YAP^{S127A} cells. **b).** Fluorescence-based quantitative soft agar assay showing the relative colony number in HOSE-MXIV, HOSE-YAP and HOSE-YAP^{S127A} cells. **c)** Soft agar assay showing colony formation in TOV21G-MXIV, TOV21G -YAP and TOV21G -YAP^{S127A} cells. **d)** Fluorescence-based quantitative soft agar assay showing the relative colony number in HOSE-MXIV, HOSE-YAP and HOSE-YAP^{S127A} cells. RFU: Relative Fluorescence unit.

For both graphs, each bar represents mean \pm SEM of four repeat assays. ***: $p < 0.001$ compared with control (MXIV).

Author Manuscript

Author Manuscript

Author Manuscript

Author Manuscript

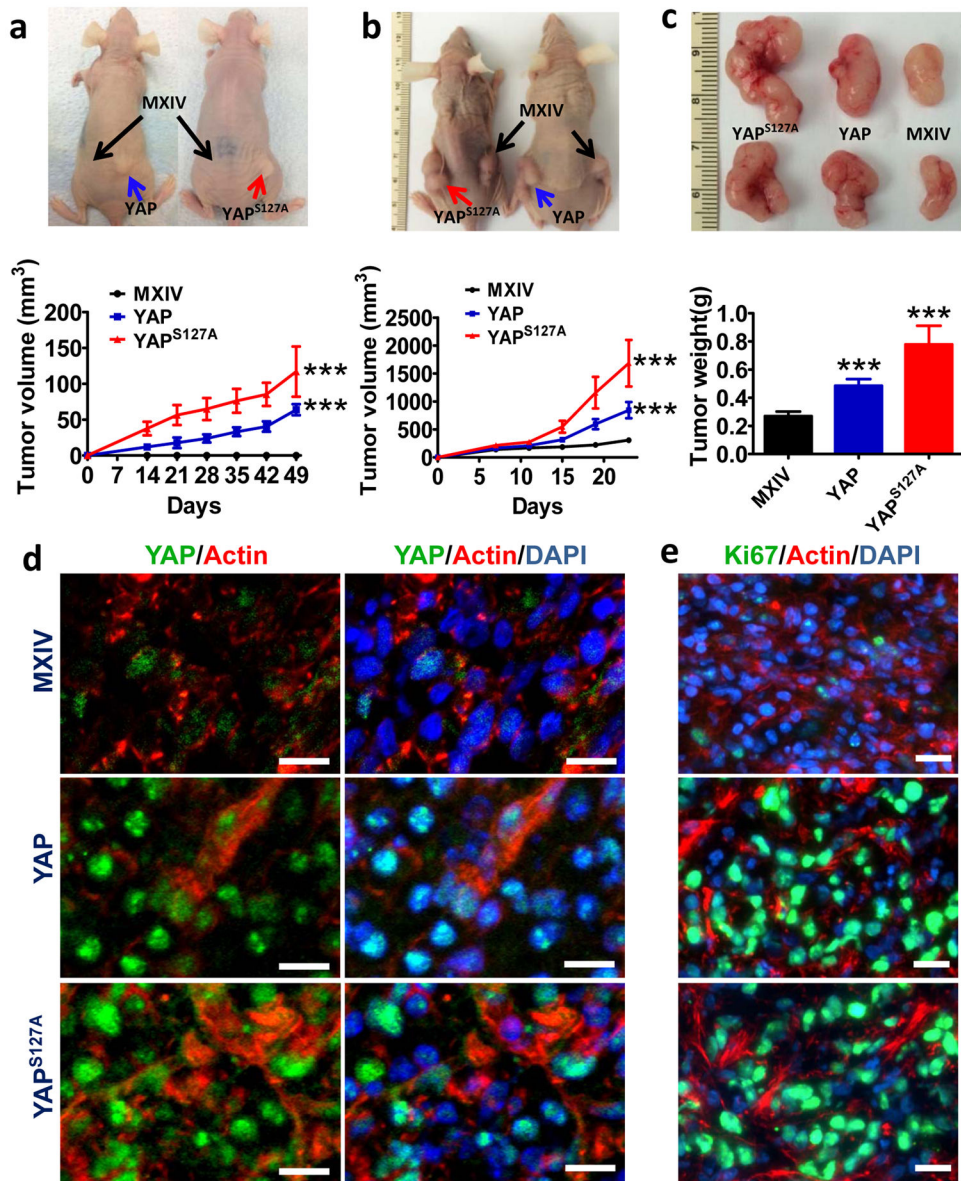


Fig. 5. Overexpression of wild type YAP or constitutively active YAP initiate tumor in immortalized human ovarian surface epithelial cells and enhance cancer cell growth in vivo
a) Top panel, representative images showing tumorigenesis in HOSE-derived cell lines (HOSE-MXIV, HOSE-YAP and HOSE-YAP^{S127A} cells) implanted into athymic nude mice. Lower panel, growth curve of tumor xenografts derived from transformed HOSE cell lines.
b) Top panel, representative images showing tumorigenesis in TOV21G-derived cell lines (TOV21G-MXIV, TOV21G-YAP and TOV21G-YAP^{S127A} cells) implanted in athymic nude mice. Lower panel, growth curve of tumor xenografts derived from TOV21G-derived cell lines.
c) Top panel: representative images of the tumor xenografts derived from TOV21G-MXIV, TOV21G-YAP and TOV21G-YAP^{S127A} cells. Lower panel: the weight of tumors derived from YAP-transfected TOV21G cells. For all representative graphs, each point or bar represents mean \pm SEM ($n = 10$ for control; $n = 5$ for YAP and YAP^{S127A}). ***: $P < 0.001$

compared with control (MXIV). **d)** Immunofluorescent histochemical analysis to determine the expression of YAP (green) in the tumor tissue derived from TOV21G-MXIV, TOV21G-YAP and TOV21G-YAP^{S127A} cells. **e)** Immunofluorescent histochemical analysis to determine the expression of Ki67 (green) in the tumor tissue derived from TOV21G-MXIV, TOV21G-YAP and TOV21G-YAP^{S127A} cells. Nuclei were stained with DAPI (blue) and actin was stained with Phalloidin-rhodamine (Red) in both d) & e). Scale bar: 10 μ m.

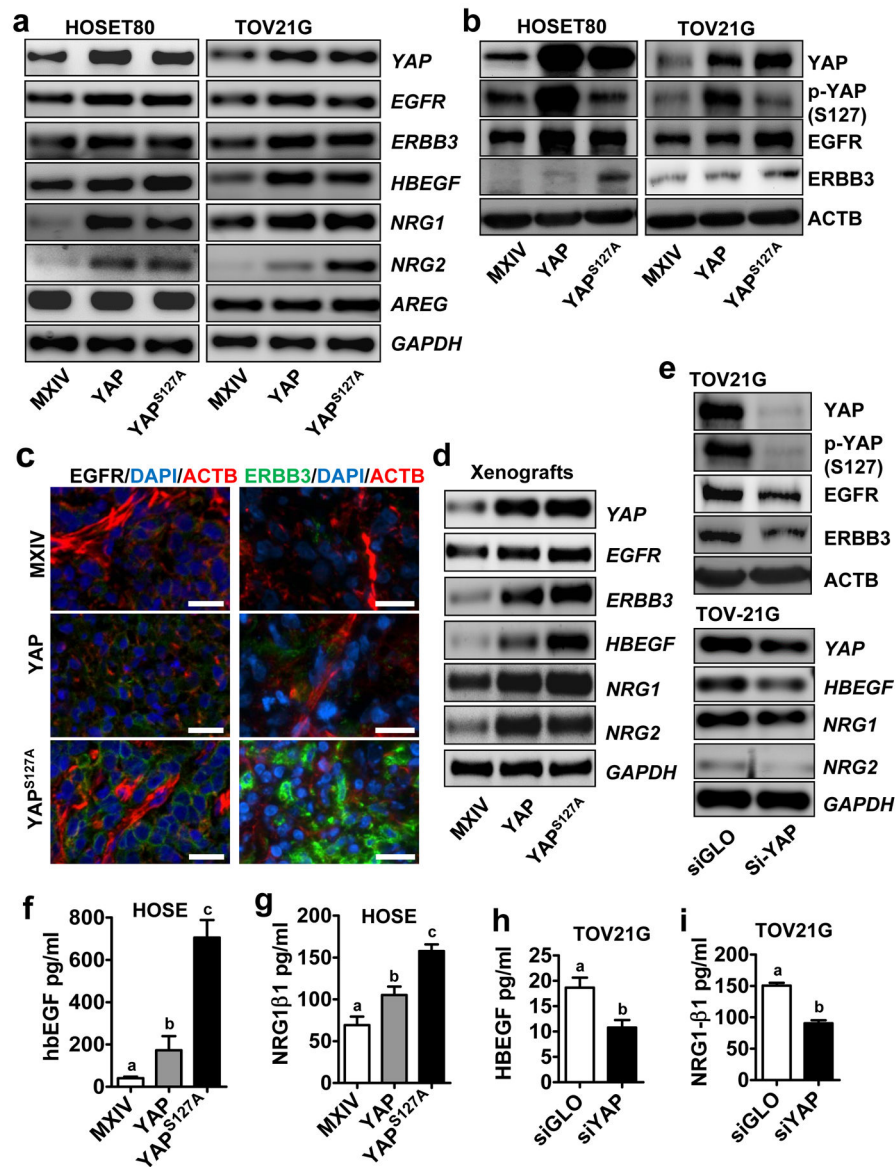


Fig. 6. YAP regulates expression of EGF-like ligands and ERBB receptors

a) Determine the mRNA expression of *NRG1*, *NRG2*, *HBEGF*, *EGFR* and *ERBB3* in HOSE-MXIV, HOSE-YAP and HOSE-YAP^{S127A} cells (left panel), and in TOV21G-MXIV, TOV21G-YAP & TOV21G-YAP^{S127A} cells (right panel) using RT-PCR. **b)** Determine protein levels of YAP, phosphorylated YAP [p-YAP (S127)], EGFR, and ERBB3 in HOSE-MXIV, HOSE-YAP and HOSE-YAP^{S127A} cells (left panel), and in TOV21G-MXIV, TOV21G-YAP & TOV21G-YAP^{S127A} cells (right panel). **c)** Determine the expression of EGFR (left, green) and ERBB3 (right, green) in xenograft tumors derived from the TOV21G-MXIV, TOV21G-YAP & TOV21G-YAP^{S127A} cell lines using Fluorescent immunohistochemistry. Actin was stained with rhodamine-phalloidin (red). Nuclei were stained with DAPI (blue). Scale bar: 20μm. **d)** mRNA levels of *ERBB1*, *ERBB3*, *HBEGF* and *NRGs* in the tumor xenografts derived from TOV21G-MXIV, TOV21G-YAP, and

TOV21G-YAP^{S127A} cells. **e)** Top panel: Western blot analysis to detect the expression of YAP, EGFR and ERBB3 protein in TOV21G cells with or without YAP knockdown using YAP siRNA (si-YAP). siGLO (a non-target siRNA) was used as a negative control; Lower panel: mRNA levels of *NRG1*, *NRG2* and *HBEGF* before and after Knockdown of YAP with YAP siRNA (si-YAP). **f & g)** Concentrations of HBEGF and NRG1 β 1 in the medium of HOSE-MXIV, HOSE-YAP & HOSE-YAP^{S127A} cells. **h & i)** Concentrations of HBEGF and NRG1 β 1 in the medium of TOV21G cells transfected with non-targeting control siRNA (siGLO) or YAP siRNA (siYAP). All experiments were repeated at least three times and the representative images were presented. Bars with different letters are significantly different from each other ($p < 0.05$).

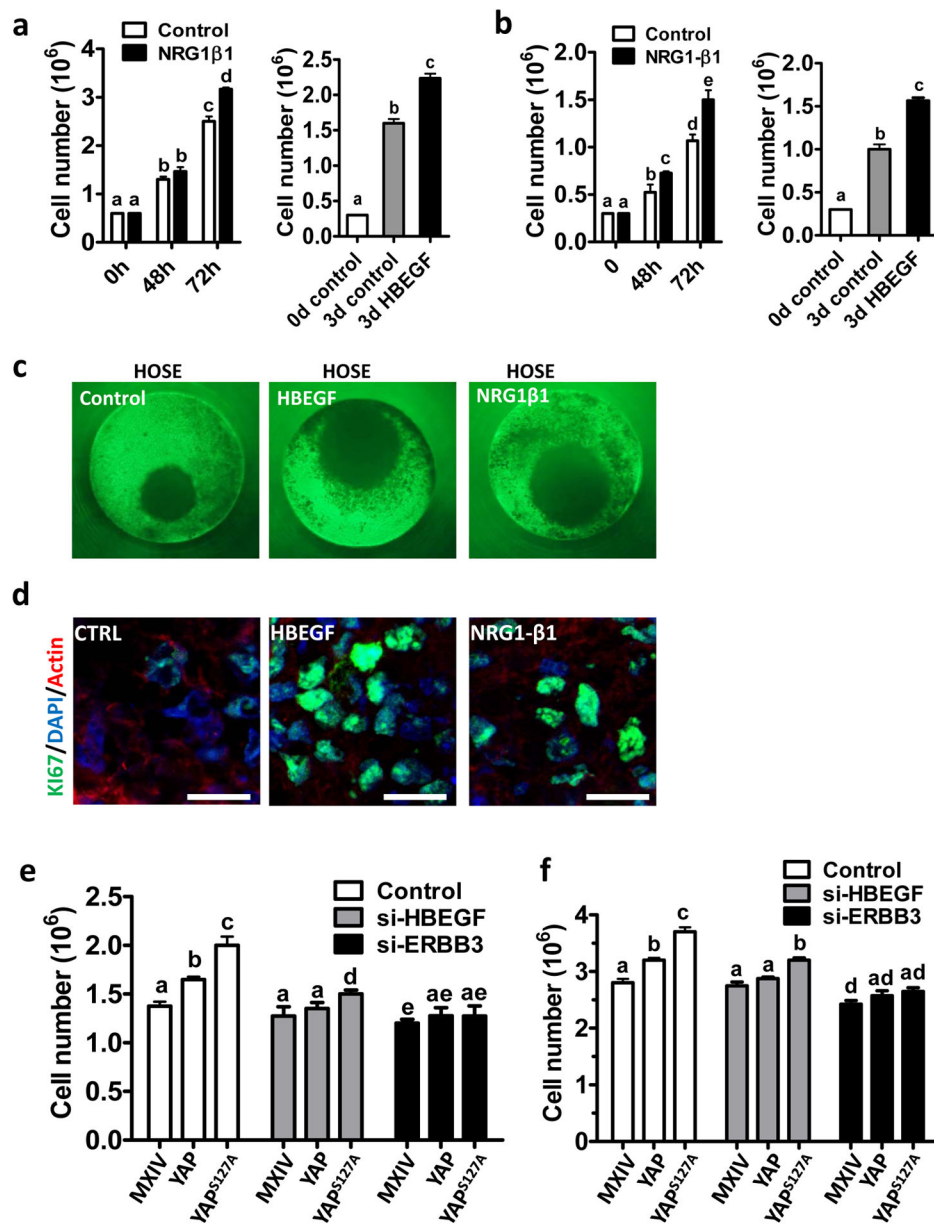


Fig. 7. ERBB3 and HBEGF are required for YAP to regulate ovarian cell proliferation
a) HBEGF and NRG1β1 stimulate proliferation of TOV21G cells; **b)** HBEGF and NRG1β1 stimulate proliferation of KGN cells; **c)** HBEGF and NRG1β1 stimulate the growth of HOSE cell in a 3D hanging drop culture system. The diameter of the well ring is 1mm. **d)** Ki67 staining (green) in the control, HBEGF-treated and NRG1β1-treated microtissues derived from HOSE cell lines. Nuclei was stained with DAPI (blue); actin was stained with rhodamin-phalloidin. Scale bar; 20μm. **e)** Knockdown of HBEGF and ERBB3 compromised YAP-stimulated HOSE cell proliferation. **f)** Knockdown of HBEGF and ERBB3 blocked YAP-stimulated TOV21G cancer cell proliferation. All experiments were repeated at least three times and the representative images were presented. Each bar in bar graphs represents

mean \pm SEM. Bars with different letters are significantly different from each other ($p < 0.05$).

Author Manuscript

Author Manuscript

Author Manuscript

Author Manuscript

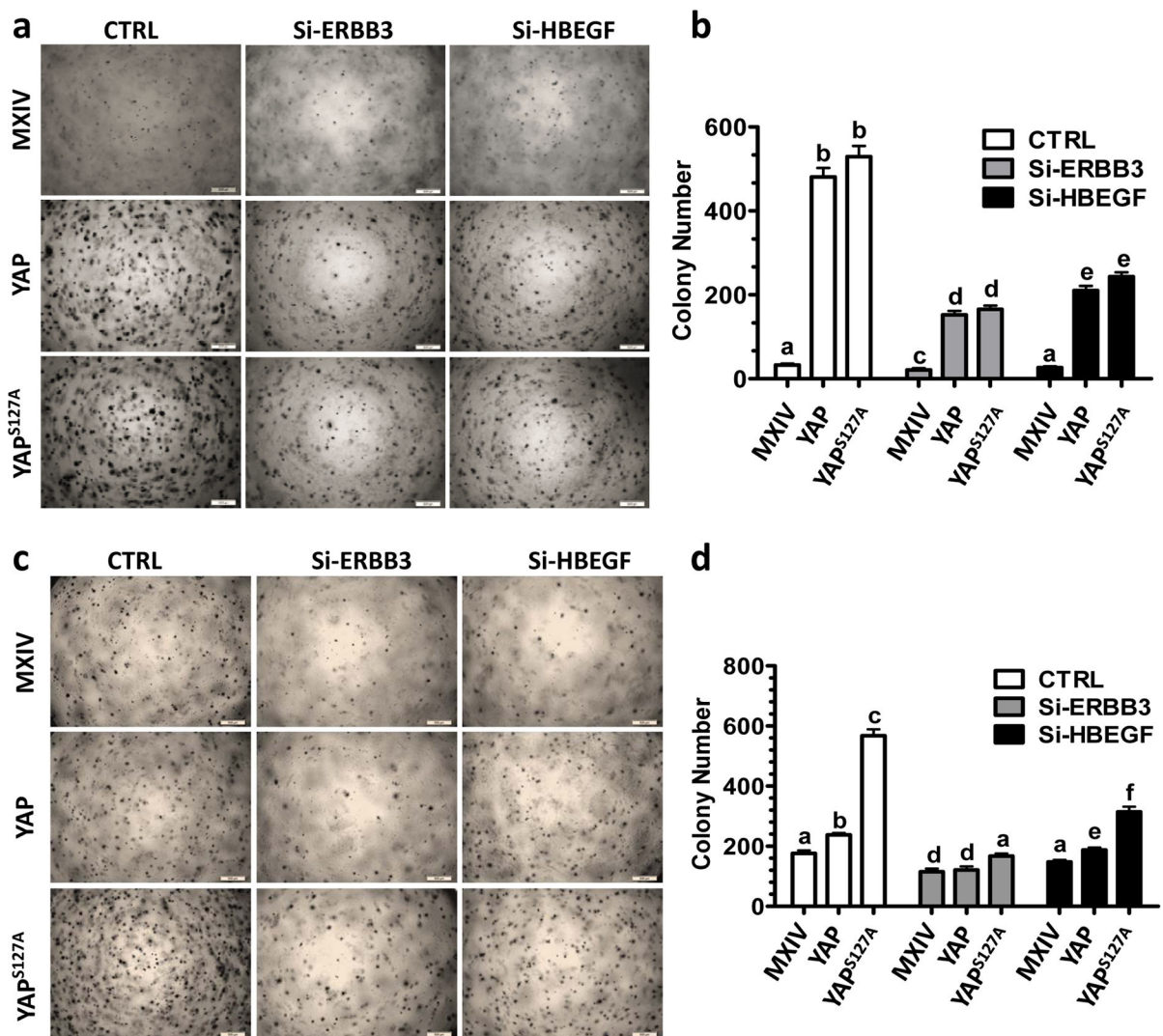


Fig. 8. ERBB3 and HBEGF are required for YAP to transform HOSE cells and enhance the anchorage-independent growth of TOV21G cells

a) Representative images showing colony formation in HOSE-MXIV, HOSE-YAP and HOSE-YAP^{S127A} cells before and after knockdown of ERBB3 and HBEGF with siRNAs. Scale bar: 500 μ m. **b)** Quantitative data showing changes of colony formation in HOSE-MXIV, HOSE-YAP and HOSE-YAP^{S127A} cells before and after knockdown of ERBB3 and HBEGF with siRNAs. **c)** Representative images showing colony formation in TOV21G-MXIV, TOV21G-YAP & TOV21G-YAP^{S127A} cells before and after knockdown of ERBB3 and HBEGF with siRNAs. **d)** Quantitative data showing changes of colony formations in TOV21G-MXIV, TOV21G-YAP & TOV21G-YAP^{S127A} cells before and after knockdown of ERBB3 and HBEGF with siRNAs. Each bar represents mean \pm SEM (n=3). Bars with different letters are significantly different from each other ($p < 0.05$).

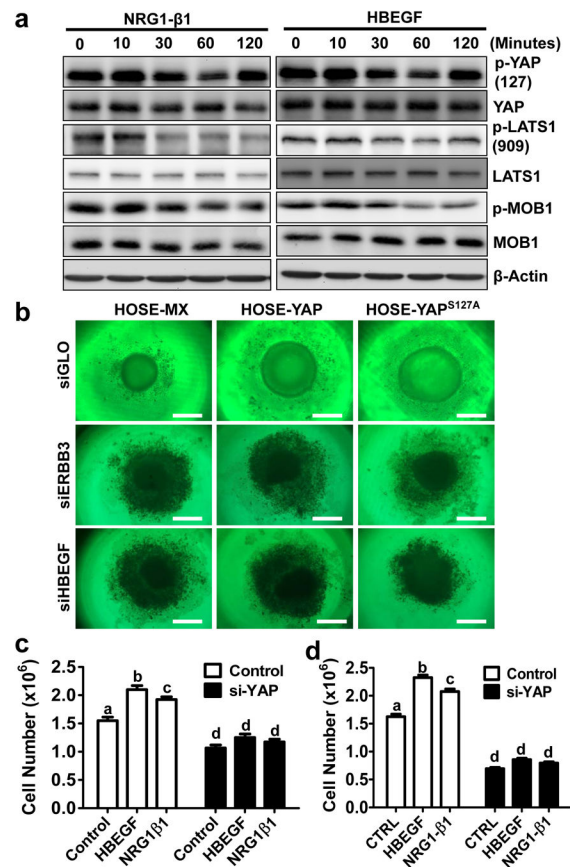


Fig. 9. The Hippo/YAP and the ERBB pathways interact with each other to regulate normal and cancerous ovarian cell growth

a) Representative Western blots showing that HBEGF and NRG1 rapidly suppress the Hippo pathway and activate YAP by dephosphorylating LATS1/2, MOB1 and YAP in TOV21G ovarian cancer cells. β -actin was used as a loading control. **b)** Knockdown of ERBB3 with ERBB3 siRNA (siERBB3), or knockdown of HBEGF with HBEGF siRNA (siHBEGF), blocks YAP-stimulated growth of spheroids derived from HOSE cell lines; **c)** Knockdown of YAP with YAP siRNA (si-YAP) totally blocked HBEGF and NRG1 induced proliferation of TOV21G cells. **d)** Knockdown of YAP with YAP siRNA (si-YAP) totally blocked HBEGF- and NRG1-induced proliferation of KGN cells. Experiments are repeated three times and representative images were presented. Each bar in bar graphs represents mean \pm SEM (n=3). Bars with different letters are significantly different from each other ($p < 0.05$).

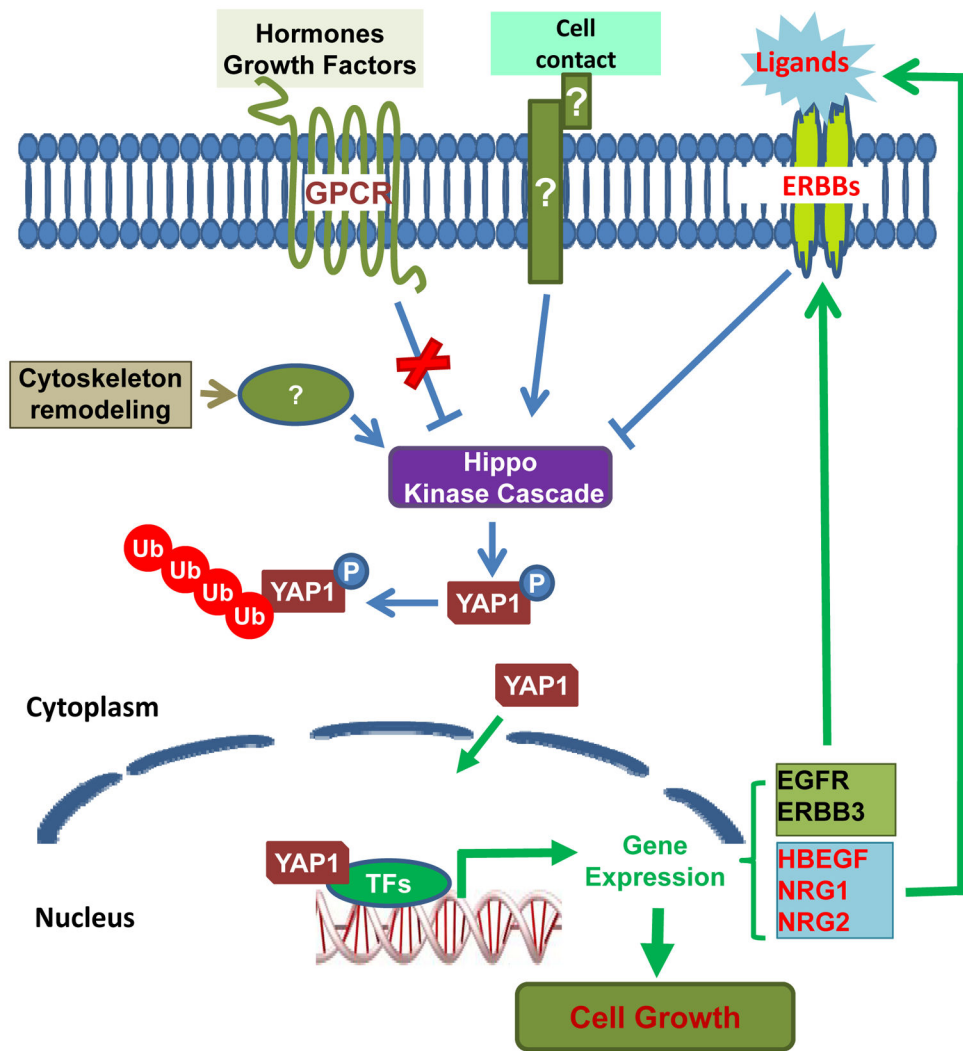


Fig. 10. A schematic diagram showing the proposed signaling pathway underlying the regulation of ovarian cancer progression by HBEGF/EGFR/YAP/HBEGF and NRG1/ERBB3/YAP/ NRG1 positive feedback autocrine loops.

Table 1

Characteristics of the human ovarian cancer patient samples

Pathology diagnosis	Tumor type	Stage (N)				Grade (N)			Total (N)	%	
		I-II		III-IV		1	2	3			Missing
		I	II	III	IV	1	2	3			
Normal	-	-	-	-	-	-	-	-	42	-	
Cancer	Clear cell	19	0	0	2	0	0	17	19	5.56	
	Mucinous	45	5	24	11	7	8	8	50	14.62	
	Endometrioid	15	6	3	10	1	7	7	21	6.14	
	Serous	188	46	34	59	105	36	36	234	68.42	
	Others	11	7	1	1	2	14	14	18	5.26	
Total		278	64	62	83	115	82	384	100.00		